Screen Print Fabricated In^{3+} Decorated Perovskite Lanthanum Chromium Oxide ($LaCrO_3$) Thick Film Sensors for Selective Detection of Volatile Petrol Vapors

Vrushali Shyamrao Shinde, Kailas Haribhau Kapadnis, Chatur Pundlik Sawant, Prashant Bhimrao Koli & Rajendra Popat Patil

Journal of Inorganic and Organometallic Polymers and Materials

ISSN 1574-1443

J Inorg Organomet Polym
DOI 10.1007/s10904-020-01660-0

Springer

Journal of Inorganic and Organometallic Polymers and Materials
https://doi.org/10.1007/s10904-020-01660-0

Screen Print Fabricated In^{3+} Decorated Perovskite Lanthanum Chromium Oxide ($LaCrO_3$) Thick Film Sensors for Selective Detection of Volatile Petrol Vapors

Vrushali Shyamrao Shinde[1,3] · Kailas Haribhau Kapadnis[2] · Chatur Pundlik Sawant[1] · Prashant Bhimrao Koli[4] · Rajendra Popat Patil[5]

Received: 23 April 2020 / Accepted: 4 July 2020

Abstract

The present work deals with the fabrication of undoped lanthanum chromium oxide and indium doped lanthanum chromium oxide material by cost effective sol–gel method. The four sensors were fabricated by screen printing technique. The indium ion concentration was varied for $LaCrO_3$ material from 0.1 M% to 0.7 M% to access the comparative gas sensing results. All the prepared materials were characterized by XRD, SEM, EDAX, TEM and IR to confirm their structural and chemical composition. The prepared sensors viz. 0.1 M% In^{3+} doped $LaCrO_3$, 0.3 M% In^{3+} doped $LaCrO_3$, 0.5 M% In^{3+} doped $LaCrO_3$ and 0.7 M% In^{3+} doped $LaCrO_3$ were investigated for gas sensing mechanism for selected gases such as petrol vapours, ethanol, ammonia, NO_2, H2S and CO_2 gases. The optimum response was recorded for tested gases for all the prepared sensors. The 0.3 M% In^{3+} doped $LaCrO_3$ found to be exceptional for petrol vapour and highest response was recorded for petrol vapors for 0.3 M% In^{3+} doped $LaCrO_3$ thick film sensor. All the indium doped are found to be good sensors for petrol vapours and moderate for other tested gases. The prime parameters for the sensors such as selectivity, response and recovery and reproducibility were recorded for the prepared sensor. The response and recovery was very rapid for 0.3 M% In^{3+} doped $LaCrO_3$ sensor. The gas sensing mechanism for petrol vapours has been established for 0.3 M% In^{3+} doped $LaCrO_3$ sensor via hole accumulation layer mechanism.

✉ Vrushali Shyamrao Shinde
vrushali.inorg1988@gmail.com

[1] Nano Chemistry Research Laboratory, Department of Chemistry, Gajmal Tulshiram Patil Arts, Science, and Commerce College Nandurbar, Affiliated to Kavayitri Bahinabai Chaudhari North Maharashtra University, Jalgaon 425412, MH, India

[2] Research Centre in Chemistry and PG Department of Chemistry, Loknete VyankatraoHiray Arts, Science, and Commerce College Panchavati, Affiliated toSPPU, Pune, MH, India, Nashik 422003, India

[3] Department of Chemistry, K.R.T Arts, B.H. Commerce and A.M. Science, College of Nashik, Affiliated to SPPU, Pune, MH, India, Pune, MH 422003, India

[4] Department of Chemistry, Arts, Commerce and Science College, Affiliated to SPPU, Pune, MH, India, Nandgaon, Nashik 423106, India

[5] Department of Chemistry, Bhosala Military College, Affiliated to SPPU, Pune, MH, India, Nashik 422005, India

Published online: 15 July 2020

Graphic Abstract

The Schematic abstract exhibits the synthesis of In-doped $LaCrO_3$ (0.1M%. 0.3M%, 0.5M% and 0.7M %) by the sol-gel manner. It also illustrates the characterization and optimal gas response to volatile petrol vapors among all the gases.

Schematic of In^{3+}-doped $LaCrO_3$ sensor with various concentrations

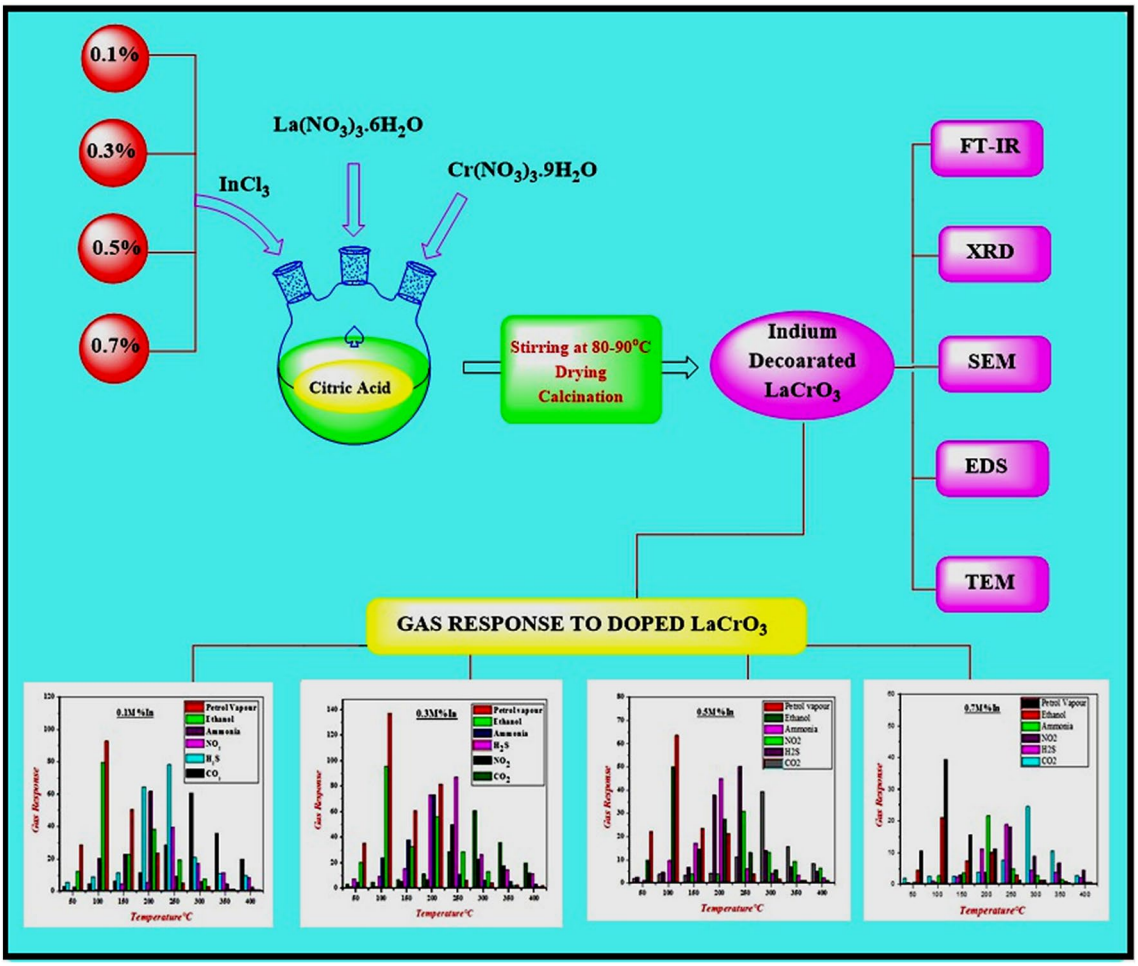

Keywords Petrol vapor sensor · In^{3+} doped $LaCrO_3$ · Gas sensors · SEM · TEM

1 Introduction

Material science is an emerging and versatile field now days with excellent applications in almost every field. The term nanotechnology and nanoscience under the heading of material science has marvelous applications in the field of catalysis. Although the materials are categorized into various types and depending upon the applications are also adopted. Among the various classes of material the perovskite category is remarkably studied and applied in to various applications such as electrochemical applications, piezoelectric sensors, SOFC, optoelectronics, surface chemistry, LED, biochemical processes, drug delievery and sensors, transducers, organic conversions etc.[1–7]. The twenty-first century has a splendid model when various researchers have attempted to make nano-materials having staggering steadiness, multifunctional properties and tremendous applications in the field of the gas sensor, identifying to perceive and screen the diverse toxic gases/fumes, released from ventures and distinctive sources century has a splendid model when various researchers have attempted to make nano-materials having staggering steadiness, multifunctional properties and tremendous applications in the field of the gas sensor, identifying to perceive and screen the diverse toxic gases/fumes, released from ventures

and distinctive sources. The release of chemical pollutants from the industries, automobiles and domestic into the atmosphere is constantly causing problems such as acid rain, global greenhouse effect and ozone depletion etc. Pollutants in the atmosphere are caused by hazardous and toxic gases from automobile and industrial exhaust. Many types of gases have been used as raw materials in recent years in various sectors of industry. If there is a question with leakage, it is essential to control these gases so that damage to property and human life is at low risk. Public health is indirectly affected by the deposition of air pollutants in the environment and ingestion of plants and animals, resulting in chemicals entering the food chain or drinking water and thus creating additional sources of human exposure. Also, the structure and functioning of ecosystems are influenced by the direct effects of air pollutants on plants, animals and soils, including their self-regulatory capacity, thereby affecting the quality of life.

In recent years, nanostructured metal oxide semiconductors (MOS) have attracted great interest due to their novel properties and variety of applications. One of the most important applications of such MOS is in the field of gas sensing. Gas sensors are widely used industrially as civilian applications for detecting and monitoring toxic, hazardous and combustible gases. This directly helps in maintaining human health as well as climate safety. Two types of metal oxide sensors have been studied extensively to date to detect and monitor these types of hazardous gases. The most commonly used n-type are MOS, ZnO, Fe_2O_3, In_2O_3, SnO_2, WO_3 and p-type MOS, CuO, NiO, CO_3O_4 and $LaCrO_3$ etc. [8].

Records of some of the most notorious deadly accidents: Bhopal (M.P.), methyl isocyanate (MIC) gas from the Indian Gas Disaster Union Carbide Limited plant storage tank on the night of December 2–3, 1984. Approximately 2 lakh residents were affected by toxic MIC gas leakage in a single incident of the Bhopal gas tragedy. The gas explosion incident reported from Terrible Gas Cracker Project Blast at Nagothane (5 November 1990) in Konkan, MH, India. There are many incidents of cooking gas explosions (LPG) in kitchens reported around the world, as well as the petrol vapours (gasoline) leakage is also responsible for many incidents reported in recent years. There are many non-communicable diseases like oxidative stress, haematotoxicity, cancer, cardiovascular diseases (CVD, 31%), chronic lung disease, respiration and breathing related disease are reported due to consumption of toxic gas vapours. Environmental factors, especially air pollution, pose additional risks with underestimated health implications in the Global Burden of Disease (GBD). Long-term exposure to enhanced cellular substances impairs vascular function, leading to myocardial infarction, arterial hypertension, stroke and heart failure. The main sources of sensitive particles are fossil fuel and biomass combustion, industry, agriculture, and air-borne dust [9, 10].

The petroleum refining right from crude petroleum processing to the complete gasoline formation there many critical processes operated with petrol and similar products. There are many applications of petrol like used as thinner, industrial solvents, decorative agents, hence during these application the consumption of the petrol vapours is at high riks. The transportation is another difficult task to carry petroleum products from one place to another place from particular industries, enhances many critical risks. Hence the demand of petrol vapour sensor is obvious, due to many critical risks of petrol vapours. However the research community is working hard to develop excellent petrol vapour sensors based on semiconducting material thick/thin film sensors technology. There are many research papers have been reported on the traditional gas sensing such as HN_3, NO_2, SO_2,CO_2, H_2S, LPG, Methane, methanol, ethanol, acetone, H_2 etc. But very rare research work has been reported for petrol vapour sensing. Hence our main focus over this project was to report the detail study of petrol vapor sensing. The perovskite oxide is efficient sensors to sense the many gases like CO, CO_2 etc. The undoped perovskite $LaCrO_3$, was employed to sense many gases, here indium doped $LaCrO_3$ sensor applied for the petrol vapours sensing in addition to other gases in this research work [11–20].

Traditionally the undoped semiconducting metal oxide based sensors are largely utilized to sense the different gases. But, from last decade trend is refashioned, where the doping of the metal or non-metal over the selected oxide is demanding. The main purpose behind the doping is to decline the band gap energy and enhance the porosity and surface area of undoped material. Hence in the present research we doped the indium metal over the $LaCrO_3$ lattice. The undoped $LaCrO_3$ and indium doped $LaCrO_3$ has been investigated for comparative study. The indium ion concentration from 0.1 M%, 0.3 M%, 0.5 M%, 0.7 M% was incorporated over the $LaCrO_3$ material via sol–gel in-situ doping method. These all sensors with varied concentration of indium ion doped $LaCrO_3$ was investigated for gas sensing of gases such as H_2S, NH_3, C_2H_5-OH, petrol vapors, CO_2 and NO_2 gases. Out of these all sensors the 0.3 M% In^{3+} doped thick film $LaCrO_3$ showed maximum response for petrol vapours. Among the important characteristics of the sensor such as selectivity, gas response, response and recovery, reusability and gas sensing mechanism of petrol vapour for indium doped $LaCrO_3$ has been established. In this research work all the sensors with varied indium concentration for $LaCrO_3$ sensor with petrol vapour is investigated in detail and comparative reports of undoped and indium doped $LaCrO_3$ sensor has been presented.

2 Methods and Materials

2.1 Material

The indium (In^{3+}) doped $LaCrO_3$ nanoparticles were prepared from the chemicals without further purification. The chemicals used are Lanthanum nitrate La $(NO_3)0.6H_2O$, Chromium nitrate $Cr(NO_3)_3$. $9H_2O$, $InCl_3$ and Citric acid analytical grade were purchased from Alfa Asser, Mumbai.

2.2 Sol–Gel Synthesis of Nanostructure Indium Doped $LaCrO_3$

Here, the nanostructured 0.1 M% In^{3+} doped $LaCrO_3$ nanoparticles were fabricated by the cost effective sol–gel method. The mixture of lanthanum nitrate [La $(NO_3)_3$], chromium nitrate [Cr $(NO_3)_3$], Indium chloride and citric acid were used. The calculated amount of lanthanum nitrate 4.325 g, chromium nitrate 3.996 g, indium chloride 0.0022 g, and 1.72 g citric acid all were dissolved in 100 ml distilled water with continuous stirring on the magnetic stirrer, heated at 80–100 °C, to evaporate distilled water for at least 2 to 3 h. A homogeneous thick gel of the above mixture was obtained. This gel was decomposed by direct heating. The gel initially began to swell and stuffed to the beaker producing a frothy precursor. This froth includes pieces of extremely small particle size. These hard particles crushed finely with mortar and pestle and annealed for 5–6 h at around 550 °C. The green colour fine powder of 0.1 M% In^{3+}doped $LaCrO_3$ are obtained. Similar procedure was repeated for the preparation of 0.3 M% In^{3+} doped $LaCrO_3$, 0.5 M% In^{3+} doped $LaCrO_3$ and 0.7 M% In^{3+} doped $LaCrO_3$ nanostructures [21, 22].

2.3 Characterization

The X-ray diffraction pattern for undoped $LaCrO_3$ and In^{3+}doped $LaCrO_3$ was recorded with the aid of X-ray diffractometer Cu/40 kV/40 mA, from Goniometer Ultima IV and x-ray diffractometer [Bruker D8, Advance, Germany] using CuKα radiation ($\lambda = 1.5409$ A^0).The surface characteristics and morphology of prepared undoped and doped $LaCrO_3$ were investigated by scanning electron microscope with EDAX (FEI NOVA SEM 450).The crystal structure investigation of prepared material was analyzed by transmission electron microscope (TEM) model number S-JEOL/JSM 2100. FTIR characterization was studied on Shimadzu IR-affinity 1S. Gas sensing measurement were performed by using a conventional static gas sensing unit as represented in Fig. 1

2.4 Fabrication of In^{3+}Doped $LaCrO_3$ Thick Films by the Conventional Screen-Printing Method

2.4.1 Fabrication of Thick Film Sensor of Undoped $LaCrO_3$ Nanomaterial

The thick film transducer of synthesized undoped $LaCrO_3$ nanoparticles was prepared with the aid of screen printing technique. For thick film sensor preparation, the inorganic to organic ration was maintained as 70: 30 respectively. In this case the inorganic part comprises undoped $LaCrO_3$ nanomaterial, while organic part comprises 92% ethyl cellulose (EC), 8% butyl carbitol acetate (BCA). By keeping definite inorganic and organic ratio of all these materials were mixed together in mortar and pestle (previously washed and dried by acetone). This mixture was crushed for at least 20–25 min until thixotropic phase (paste like)

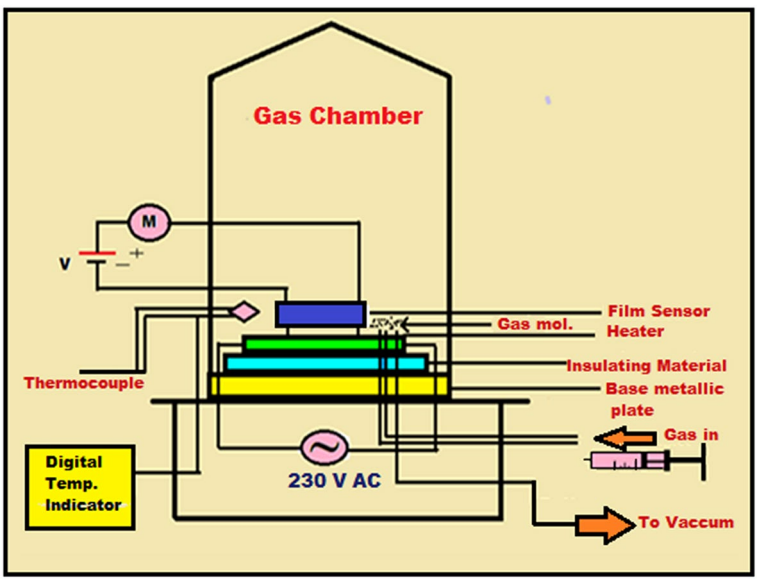

Fig. 1 Gas sensing apparatus block diagram utilized in present study

was achieved (psedoplastic mass). After this paste formation, it was applied on antecedent cutted glass substrate film (2 × 1 cm) by screen printing method. The screen of nylon (mesh number 355, 40 S) was prepared for this technique. The appropriate mask size was created over the screen by photolithography technique. After complete coating of the films, the films were dried at room temperature for twenty minutes, thenceforth, the coated films were dried under infra-red lamp for thirty minutes. Finally coated films were calcined under m uffle furnace for 550 °C for three hours. The undoped $LaCrO_3$ thick films now ready for characterization, electrical and gas sensing study [23].

2.4.2 Fabrication of Thick Film Sensor of 0.3 M% In^{3+} Doped $LaCrO_3$ Nanomaterial

The thick film transducer of synthesized 0.3 M% In^{3+} doped $LaCrO_3$ was prepared with the aid of screen printing technique. For thick film sensor preparation, the inorganic to organic ration was maintained as 70:30 respectively. In this case the inorganic part comprises 0.3 M% In^{3+} doped $LaCrO_3$ nanomaterial, while organic part comprises 92% ethyl cellulose (EC), 8% butyl carbitol acetate (BCA). By keeping definite inorganic and organic ratio of all these materials were mixed together in mortar and pestle (previously washed and dried by acetone). This mixture was crushed for at least 20–25 min until thixotropic phase (paste like) was achieved (psedoplastic mass). After this paste formation, it was applied on antecedent cutted glass substrate film (2 × 1 cm) by screen printing method. The screen of nylon (mesh number 355, 40 S) was prepared for this technique. The appropriate mask size was created over the screen by photolithography technique. After complete coating of the films, the films were dried at room temperature for twenty minutes, thenceforth, the coated films were dried under infra-red lamp for thirty minutes. Finally coated films were calcined under muffle furnace for 550 °C for three hours. The 0.3 M% In^{3+} doped $LaCrO_3$ thick films now ready for characterization, electrical and gas sensing study.

2.4.3 Fabrication of Thick Film Sensor of 0.5 M% In^{3+} Doped $LaCrO_3$ and 0.7 M% In^{3+} Doped $LaCrO_3$ Nanomaterial

Same method is followed as mentioned above for the preparation of thick film sensor of 0.5 M% In^{3+} doped $LaCrO_3$ and 0.7 M% In^{3+} doped $LaCrO_3$ nanomaterial. The difference was for inorganic ratio, the inorganic ratio was considered for 0.5 M% In^{3+} doped $LaCrO_3$ and 0.7 M% In^{3+} doped $LaCrO_3$ nanomaterial. The remaining overall procedure was same for preparation of these sensors in comparison to the undoped $LaCrO_3$ thick film sensor.

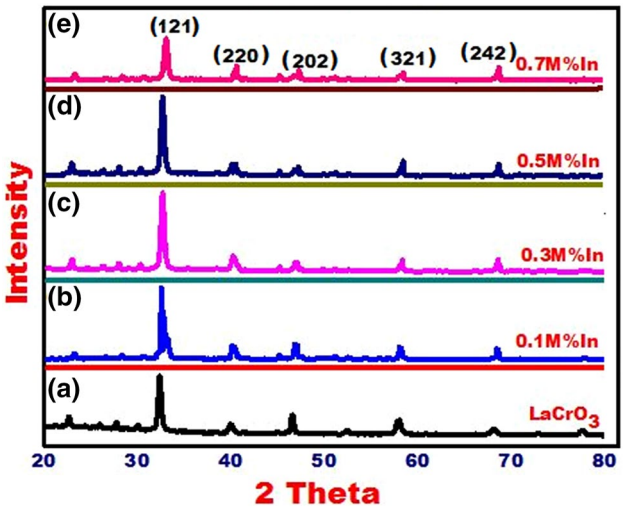

Fig. 2 (a) XRD spectrum of undoped LaCrO3 nanostructure (b–d) 0.1 M% In^{3+}—0.7 M% In^{3+} doped $LaCrO_3$ nanostructure

3 Results and Discussion

3.1 Characterization of In^{3+} Doped $LaCrO_3$ (0.1 M%, 0.3 M%, 0.5 M% and 0.7 M%)

3.1.1 X-ray Diffraction

The X-ray diffraction pattern for undoped $LaCrO_3$ and various concentration of In^{3+} doped $LaCrO_3$ is shown in Fig. 2

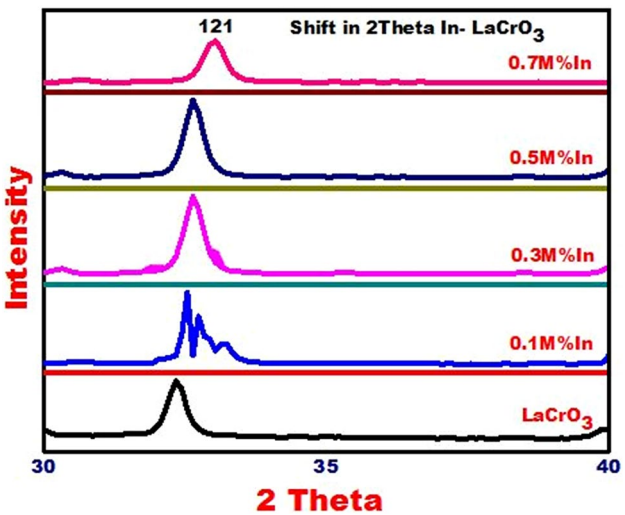

Fig. 3 shift in 2 theta at 121 planes of In^{3+} doped LaCrO3 nanostructure from concentration of 0.1 M% to 0.7 M%

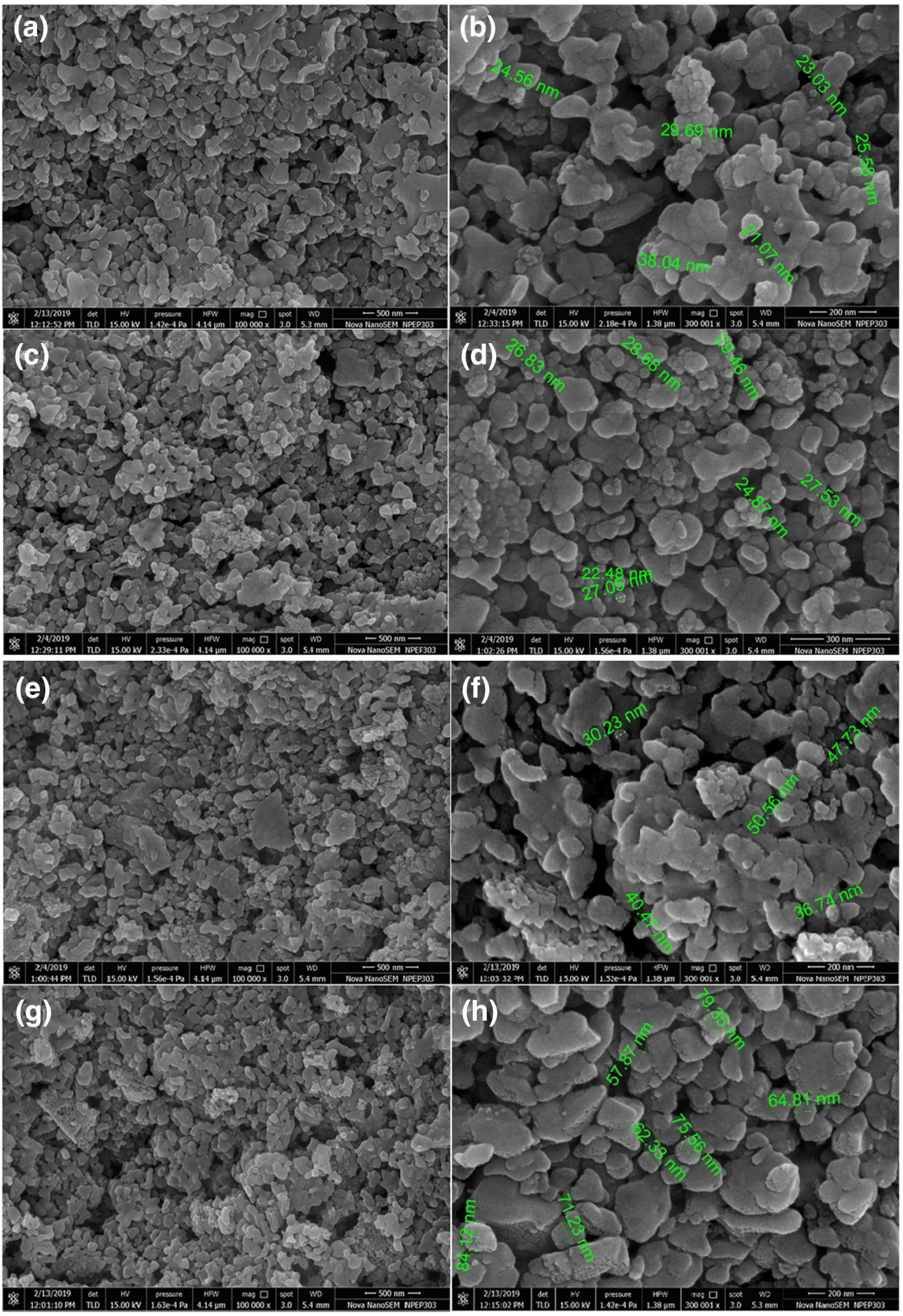

◂**Fig. 4** **a**, **b** SEM images of 0.1 M% In^{3+} doped $LaCrO_3$, **c**, **d** SEM images of 0.3 M% In^{3+}doped $LaCrO_3$ (**e**, **f**), SEM images of 0.5 M% In^{3+}doepd $LaCrO_3$, **g**, **h** 0.7 M% In^{3+}doped $LaCrO_3$

where the observed diffraction peaks correlated well with reported data of $LaCrO_3$ (JCPDS Card No. 33-0701). From X-ray diffraction data it was concluded that the prepared $LaCrO_3$ material belongs to orthorhombic phase, which is most often crystal phase for lanthanum chromium oxide. The strong and intense peak of the XRD spectrum designates better crystallinity with preferred orientation along the (121) plane for undoped $LaCrO_3$ and In^{3+} doped $LaCrO_3$ material. Further, it was observed in XRD spectrum of Indium doped $LaCrO_3$, as the amount of indium ion (In^{3+}) is enhanced from 0.1 to 0.7 M%, the diffraction peak (121) is shifted towards a higher angle of 2θ, shown in Fig. 3. The average crystallite size calculated by Debye-Scherer Eq. (1)

$$D = K\lambda/\beta \cos\theta \tag{1}$$

where λ is the radiation of wavelength (1.54 A^0), β is FWHM (Full-Width Half wave Maxima), θ is the Bragg angle in degree, K is constant ranges between 0.9 to 1 and D is the average crystallite size. The average crystallite size of undoped $LaCrO_3$ calculated as 13.04 nm. But the grain size for doped nanostructures gets slightly increased. Typically for 0.1 M% In^{3+} doped $LaCrO_3$ size found to be 31.24 nm, for 0.3 M% In^{3+} doped $LaCrO_3$, it found to be 33.09 nm, for 0.5 M% In^{3+} doped $LaCrO_3$ size found to be 35.12 nm and for 0.7 M% In^{3+} doped $LaCrO_3$ size found to be 35.28 nm. As per the literature reports, as the dopant concentration added in base material, the grain size is increased [24, 25]. The electrical properties of the ABO_3 (Perovskite) type $LaCrO_3$ is enhanced by doping with divalent ion. The ABO_3 perovskite structure is flexible and has considerable vacancies either A or B site. Indium prefers B site as its ionic radii (0.80 Å) close to chromium (0.67 Å). Indium doping in $LaCrO_3$ produces p-type semiconductor [29]. Due to the substitution of indium at chromium site, a steric constraint, caused by dopant creates distortion in the unit cell of $LaCrO_3$ perovskite structure and hence the crystallite size is slightly increased with the doping of Indium ions.

3.1.2 Scanning Electron Microscopy

Figure 4a–h shows the SEM micrograph of differential magnified top vision of doped $LaCrO_3$ thick films with varying concentrations of indium 0.1 Mol%, 0.3 Mol%, 0.5 Mol%, 0.7 Mol%, respectively, a distinctive morphological difference is observed among these images. Micro scaled spheres of different sizes were produced by agglomeration nanoparticles in the film. The 0.3 Mol% indium doped $LaCrO_3$ film shows various sized nanoparticles particles more evenly distributed on the surface [26–28]. However, increasing concentration of indium dopants in $LaCrO_3$ initiates an increase in particle size is observed due to the ionic radii of indium slightly greater than chromium. At an appropriate concentration, indium ions can occupy chromium sites in the lattice of $LaCrO_3$. The average particle sizes of synthesized nanoparticles were observed for 0.3 M% In^{3+} from 26 to 29 nm range while a higher concentration of indium exhibit larger particles size ranging from 34 to 84 nm. From SEM images of indium doped $LaCrO_3$ nanomaterial, nearly all the SEM micrographs having homogeneous surface area, as well as in all the SEM micrographs it can be seen that the formation of smaller voids over the surface of all prepared $LaCrO_3$ nanostructures, with different indium concentration as represented in Fig. 4a–h. These types of empty space or cavities or voids plays very vital role in gas sensing mechanism, as gas sensing mechanism is adsorption phenomenon, takes place via physisorption and chemisorption. Thus voids presents on the surface of film sensor, are very effective in gas sensing studies.

3.1.3 Energy Dispersive Spectroscopy (EDAX)

Moreover, the energy-dispersive X-ray spectroscopy was used to access the elemental composition of In^{3+} doped $LaCrO_3$ with its all concentrations. Tables 1, 2, 3, and 4 represents and confirmed the presence of La, In, Cr and O with values as per synthesis and also EDX spectrum shows the various peaks for La, Cr, In and O which confirms synthesis of indium doped $LaCrO_3$ nanostructures. In the case of undoped $LaCrO_3$, the sharp peak was found at 4.8 keV for lanthanum and chromium is resoluted at 5.4 keV. While the characteristics peak of indium in each concentration was found to at 3.2 keV, while the remaining elements viz. La, Cr, O resoluted at their characteristics scale of 4.8 keV, 5.4 keV and 0.4 keV respectively as represented in Fig. 5. The results obtained for indium doped $LaCrO_3$ are in good agreements with the reported results [29] Fig. 5a–d demonstrates the EDS images of In^{3+}-doped $LaCrO_3$ nanostructures.

Table 1 Elemental Composition of 0.1 M% In^{3+} doped $LaCrO_3$

Sr. No.	Element	Atomic%	Weight%
1	Oxygen	71.20	30.20
2	Chromium	13.35	18.11
3	Lanthanum	14.22	48.38
4	Indium (0.1 M%)	1.23	3.31
	Total	100	100

Table 2 Elemental Composition of 0.3 M% In^{3+} doped $LaCrO_3$

Sr. No.	Element	Atomic%	Weight%
1	Oxygen	71.29	31.41
2	Chromium	12.19	16.86
3	Lanthanum	13.93	46.59
4	Indium (0.3 M%)	2.59	5.14
	Total	100	100

Table 3 Elemental Composition of 0.5 M% In^{3+} doped $LaCrO_3$

Sr. No.	Element	Atomic%	Weight%
1	Oxygen	70.74	30.47
2	Chromium	11.97	17.31
3	Lanthanum	13.31	46.22
4	Indium (0.5 M%)	3.98	6.00
	Total	100%	100%

Table 4 Elemental Composition of 0.7 M% In^{3+} doped $LaCrO_3$

Sr. No.	Element	Atomic%	Weight%
1	Oxygen	70.45	28.82
2	Chromium	11.91	16.96
3	Lanthanum	13.07	46.10
4	Indium (0.7 M%)	4.57	8.12
	Total	100%	100%

3.1.4 High Resolution Transmission Electron Microscopy (HR-TEM)

The high resolution transmission electron microscopy was utilized to investigate the crystal morphology and lattice structure of prepared of 0.3 M% In^{3+}dope $LaCrO_3$ nanostructures. The TEM images of 0.3 M% In^{3+}doped $LaCrO_3$ nanostructures are as depicted in Fig. 6a–c, while the selected area diffraction pattern is shown in Fig. 6d. It can be seen from the images of In^{3+}doped $LaCrO_3$ nanostructures showing the orthorhombic crystal lattice. The TEM images for indium doped $LaCrO_3$ are in good agreement with the reported data.

The varied size of indium doped $LaCrO_3$ nanostructures is in the range of 34 to 58 nm can be seen from Fig. 6a which is reliable with the results obtained from the XRD and FE-SEM dimensions. The selected area electron diffraction (SAED) were used to more explore the microstructure. Figure 6d reveals that a crystalline structure, since the bright spot appearing in SAED images can be assign to the crystallinity of the prepared material 0.3 M% In^{3+}doped $LaCrO_3$ thick film sensor.

3.1.5 Fourier Transform Infra Red Analysis (FT-IR)

Figure 7 shows FTIR spectra of In^{3+} doped $LaCrO_3$ samples from In^{3+}concentration of 0.1 to 0.7 M%. The FT-IR spectrums show the strong absorption bands relating to stretching vibrations of La–O and Cr–O at 551.67 cm^{-1} and 571 cm^{-1} respectively. The wavenumber at 1480–1550 is can be assigned to water distortion. The peak perceived at 2350–2400 is an H–O–H stretch for an adsorbed water molecule. The small peak observed at 1600–1650 cm^{-1} indicates the water of crystallization in the lattice of lanthanum chromate [29–32].

3.1.6 Gas Sensitivity, Selectivity, Response and Recovery, Reproducibility Study of In^{3+} Doped $LaCrO_3$ with Different Concentrations

The gas sensitivity for thick films of all In-doped sensors was tested by using a static gas sensing unit, the representative diagram is as shown in Fig. 1. The gas response was measured as a function of temperature in the presence of H_2S, NH_3, C_2H_5–OH, petrol vapors, CO_2 and NO_2 gases atmosphere from room temperature to 400 °C. The variation

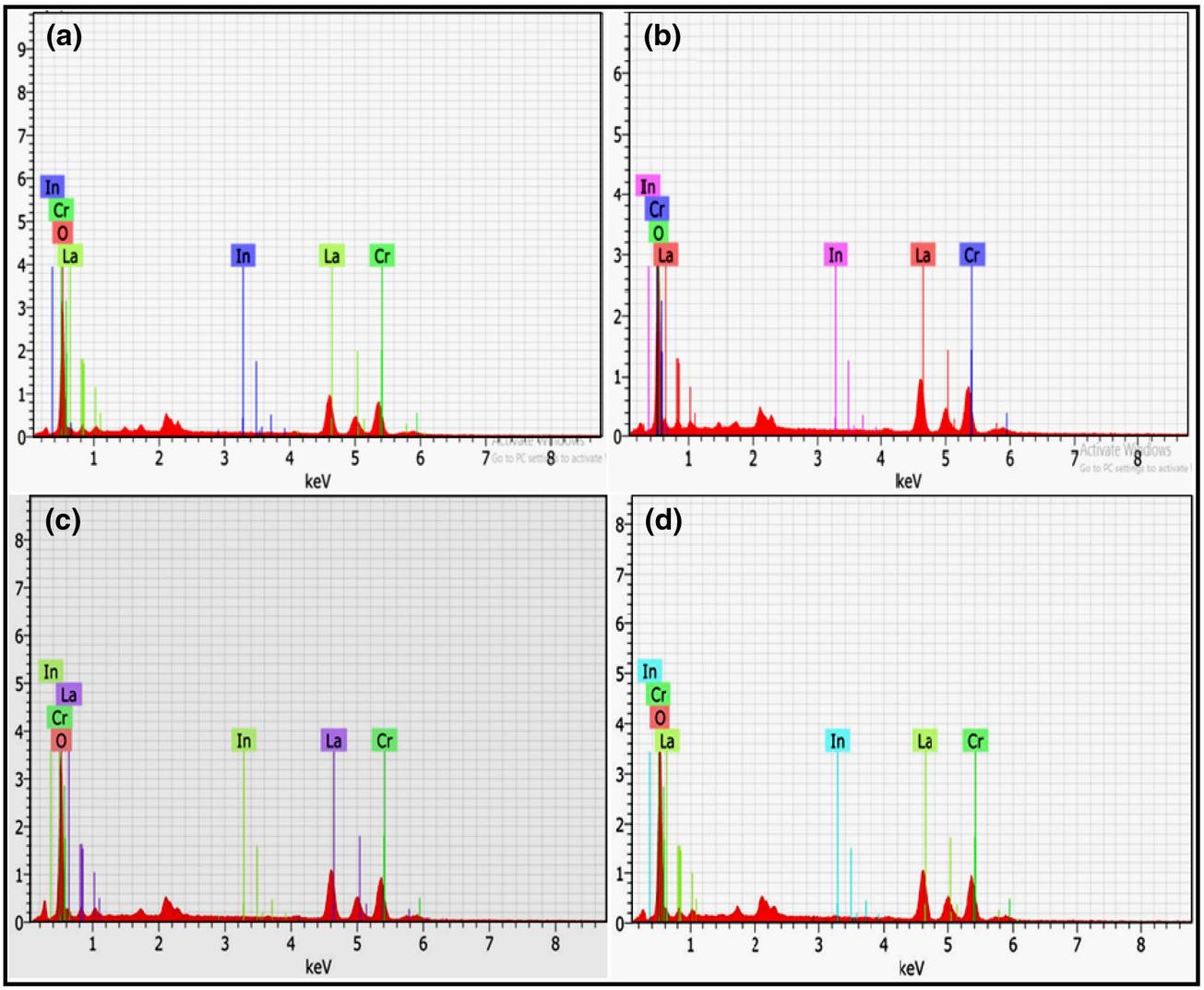

Fig. 5 EDAX images of **a** 0.1 M% In^{3+} doped $LaCrO_3$, **b**, 0.3 M% In^{3+} doped $LaCrO_3$, **c**, 0.5 M% In^{3+} doped $LaCrO_3$, **d** 0.7 M% In^{3+} doped $LaCrO_3$

resistance was measured before and after exposure of gas with the help of a digital multimeter for all In^{3+}doped sensors. The resistance of the films was estimated by utilizing output voltage digital multimeter model number ICR classic-833. At each pattern of gas presented inside the glass chamber, gas buildup was pulled back by lifting the glass chamber and fixed temperature was provided to evacuate the gas buildup of the film. The oxygenated air was permitted to go through the chamber at each gas affectability cycle. The electrical obstruction of the thick film within the sight of air (Ra), just as within the sight of gas (Rg) was estimated to ascertain the gas reaction or sensitivity (S) given by Eq. (2).

$$S\% = Ra - Rg/Ra \times 100 \quad (2)$$

where Rg is Resistance of the thick films in the presence of gas, Ra- Resistance of the thick films in the presence of gas.

The static gas system was used to investigate the influence of concentration of dopant on the gas sensing properties of thick films of 0.1 M% In^{3+} doped $LaCrO_3$, 0.3 M% In^{3+} doped $LaCrO_3$, 0.5 M% In^{3+} doped $LaCrO_3$ and 0.7 M% In^{3+} doped $LaCrO_3$ thick film sensors. The sensitivity for all sensors was tested for different gases like H_2S, NH_3, Ethanol, petrol vapors, CO_2, and NO_2 at a varied concentration of target gas such as 1000 ppm, 500 ppm, 300 ppm, and 100 ppm. The response at 1000 ppm for all gases at various concentrations of In^{3+}doped $LaCrO_3$ transducer is shown in Fig. 8a–d. In gas sensing investigation we observed that the 0.3 M% In^{3+} constructed thick film sensor sense to petrol vapors at operating temperature 100 °C and exhibits optimal gas response 137.04%. Figure 8a–d demonstrate measurement

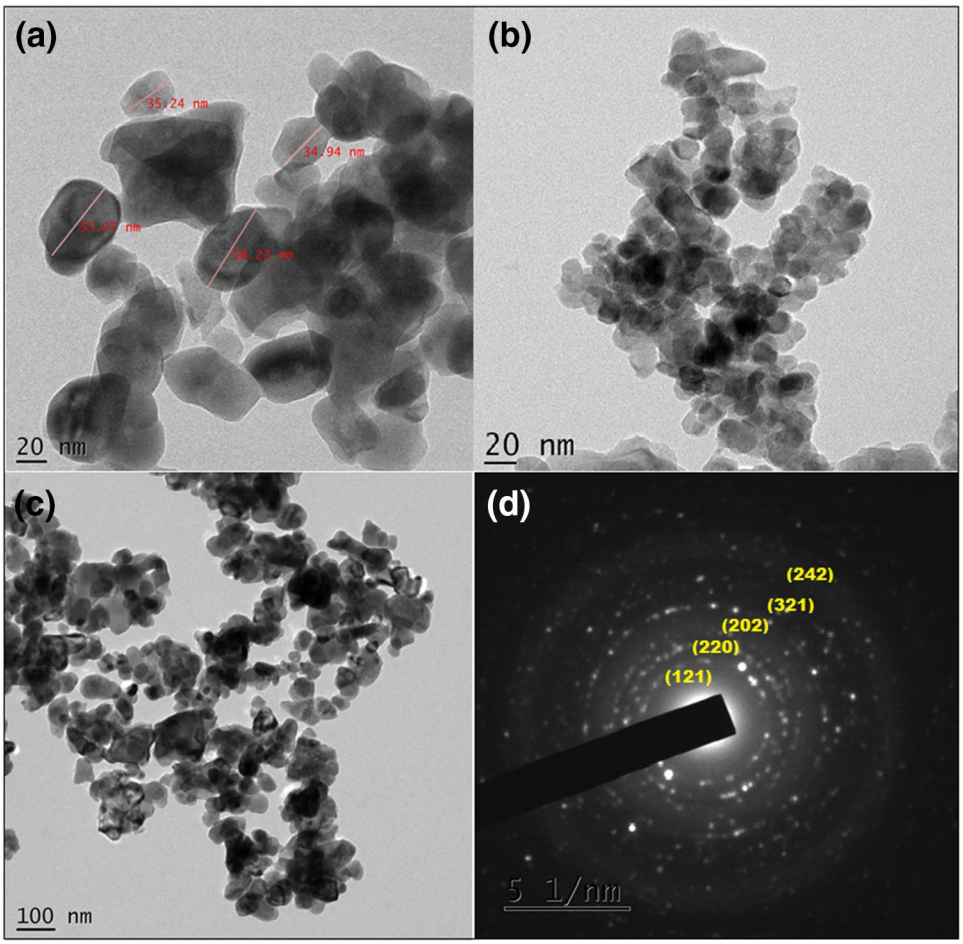

Fig. 6 **a–c** TEM images of images of 0.3 M%In^{3+} Doped with $LaCrO_3$ sensor, **d** SAED pattern of 0.3 M%In^{3+} Doped with $LaCrO_3$ sensor

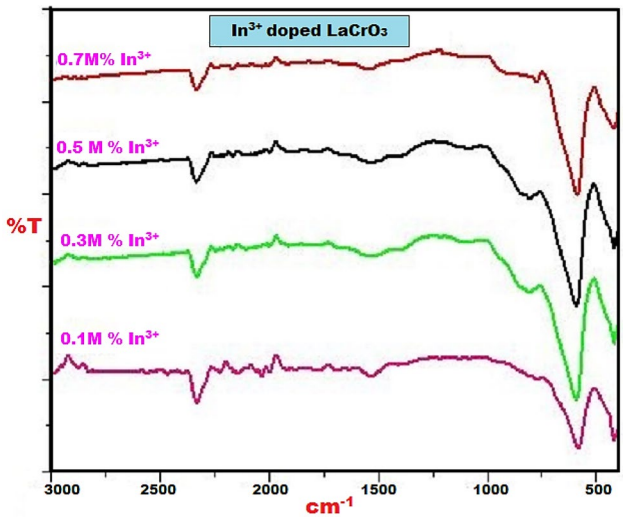

Fig. 7 FT-IR spectra of In^{3+}doped $LaCrO_3$ nanostructure with 0.1 M%, 0.3 M%, 0.5 M% and 0.7 M% concentration

of gas sensing of all samples, it was observed that up to 0.3 M% dopant concentration of In^{3+} creates more oxygen vacancies on the surface but at higher dopant concentration beyond 0.3 M% the oxygen vacancies are not enough, so the response was relatively lower. This is because the higher response may be assigned to films with more defects, optimum porosity, more oxygen vacancies and more effective surface area available for adsorption of the species of gas in case of every sensor. The gas response is also attributed to the adsorption–desorption type of sensing mechanism. It is based on the reaction between the surface of the transducer and the target gas. Several probable reactions can occur on the surface depending on the exposed target gas and the nature of semiconductor-based metal oxide sensor. Petrol vapor is reducing the type of gas which oxidized when exposed to the surface of sensing material and acts as electron donor and transfer the electrons to the thick film of p-type sensor and resistance of the film increases abruptly.

The histogram as shown in Fig. 9a–d shows the highest selectivity for petrol vapors among all the gases. All indium doped $LaCrO_3$ film sensor showed a reasonable response to petrol vapors. But 0.3 M% In^{3+} sample shows the optimum gas response of 137.04 to petrol vapors at 100 °C, while other sample shows the lower gas response in comparison

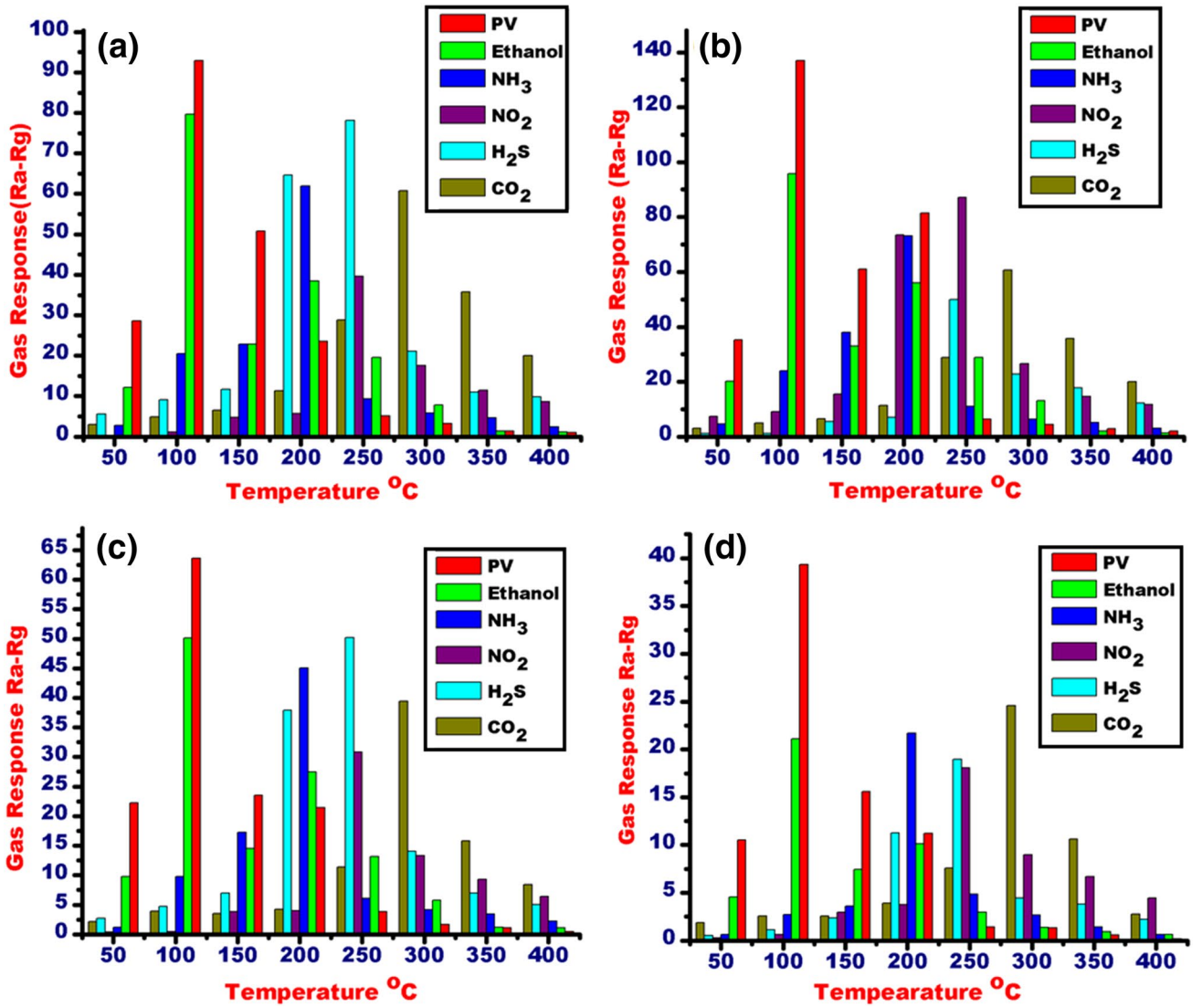

Fig. 8 **a** Gas sensing performance of 0.1 M% In^{3+}doped $LaCrO_3$ film sensor for tested gases (**b**) for 0.3 M% In^{3+}doped $LaCrO_3$ film sensor, **c** for 0.5 M% In^{3+}doped $LaCrO_3$ film sensor, **d** for 0.7 M% In^{3+}doped $LaCrO_3$ film sensor (PV = petrol vapours)

with 0.3 M% In^{3+} sample. The response gets deteriorate may be due to the inappropriate doping concentration.

The transitory response for all In^{3+} doped $LaCrO_3$ were measured by exposing 1000 ppm petrol vapors at their respective temperature as shown in Fig. 8a–d. The important parameter of every gas sensor that is response and recovery very useful for the technological utility of the sensor were measured as a function of time. The time required by a sensor to attain 90% of the maximum increase in conductance or decrease in resistance upon the exposure of the target gas is known as response time. The time taken by the sensor to get back 90% of its original resistance when the flow of gas is switched off is known as recovery time. We measured the response and recovery time of the designed sensors.

The response and recovery for petrol vapors at 0.1 M% In^{3+} doped $LaCrO_3$ sensor, 0.3 M% In^{3+} doped $LaCrO_3$ sensor, 0.5 M% In^{3+} doped $LaCrO_3$ sensor and 0.7 M% In^{3+} doped $LaCrO_3$ sensors were recorded and shown in Fig. 10a–d. For petrol vapors, the quick response was shown by 0.3 M% In^{3+} doped $LaCrO_3$ sensor at 12 s and fast recovery at 17 s. The other films also show the response time at 13 s and recovery at 21 s for 0.1 M% In^{3+}, for 0.5 M% In^{3+}, the response at 15 s and recovery at 24 s and finally 17 s response and 25 s recovery for 0.7 M% In^{3+}. From the above data and figures, we can conclude that 0.3 M% In^{3+} doped $LaCrO_3$ sample shows the best response and recovery time as compared with other samples. This quick response may be attributed due to good nanocrystalline nature and perfect doping of 0.3 M% In^{3+} into $LaCrO_3$ which may be capable

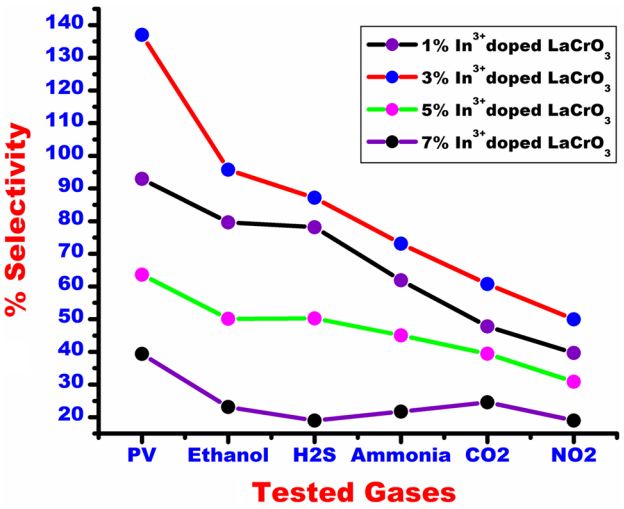

Fig. 9 Shows selectivity for petrol vapours for 1 M% In^{3+}doped $LaCrO_3$ film sensor, 0.3 M% In^{3+}doped $LaCrO_3$ film sensor, 0.5 M% In^{3+}doped $LaCrO_3$ film sensor 0.7 M% In^{3+}doped $LaCrO_3$ film sensor

of high adsorption of oxygen species onto the surface of $LaCrO_3$ by indium modification.

The reproducibility is the characteristics that take into account to confirm the stability of the sensors. We have checked this stability of all In^{3+} doped $LaCrO_3$ samples by repeating 5 gas sensing cycles up to 45 days in identical experimental conditions. We have repeated 5 gas sensing cycles at 1000 ppm gas concentration of petrol vapors for 0.3 M% In^{3+} doped $LaCrO_3$. We observed that the gas response for sensors was slightly weakened after a month. It implies no considerable variation is observed even after 45 days. From this data, it can be concluded that the stability for 0.3 M% In^{3+} doped $LaCrO_3$ is higher than other samples. The reproducibility results are as shown in Fig. 11.

3.2 Gas Sensing Mechanism

$LaCrO_3$ is a p-type MOS. The majority of charge carriers are positive holes in case p-type semiconductors. An increase in resistance is observed when the surface of p-type semiconductor comes in contact with reducing gas because targeting gas introduced negative charge into the material which reduces the concentration of holes. Exactly opposite mechanism is observed, when oxidizing gas comes in contact with metal oxide sensor surface, i.e. the resistance found to be decreased because targeting gas interacting with the surface and increased the concentration of positive holes. During the gas sensing mechanism of p-type semiconductors. The formation of HAL (Hole accumulation layer) near the surface of metal oxide semiconductors due to adsorption of oxygen anions, because of electrostatic interaction established between oppositely charged species shown in Figs. 12, 13, which developed an insulating region at cores

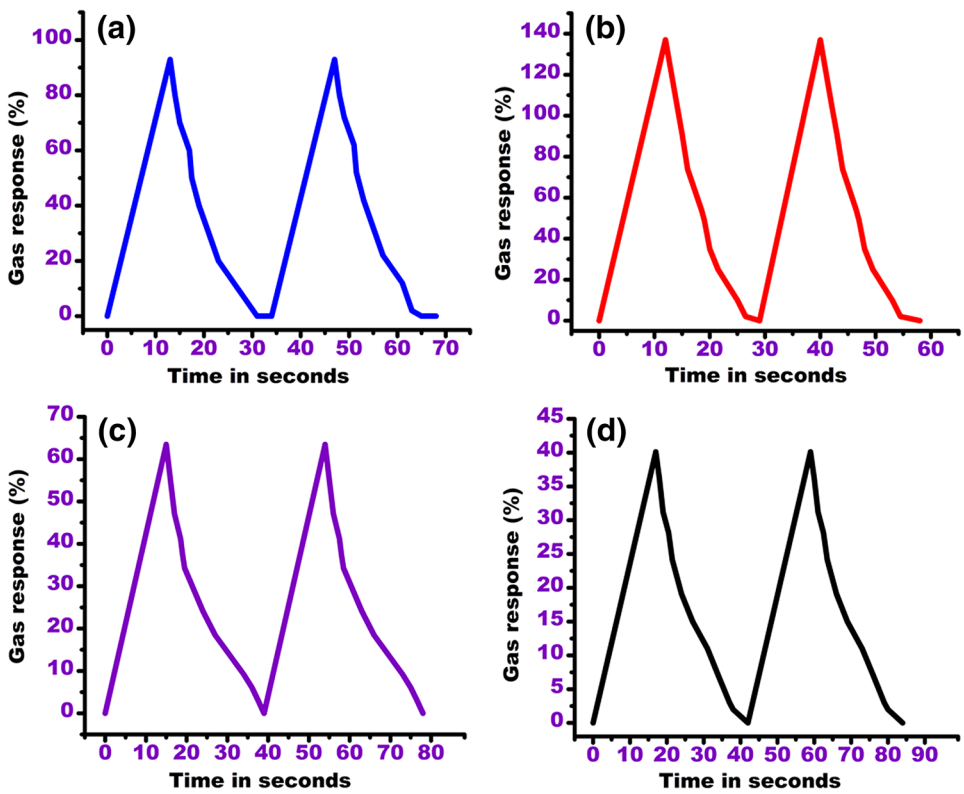

Fig. 10 **a** Response and recovery curves of petrol vapours for 0.1 M%In^{3+} doped $LaCrO_3$ sensor, **b** for 0.3 M% In^{3+} doped $LaCrO_3$ sensor, **c** 0.5 M% In^{3+} doped $LaCrO_3$ sensor, **d** 0.7 M% In^{3+} doped $LaCrO_3$ sensor

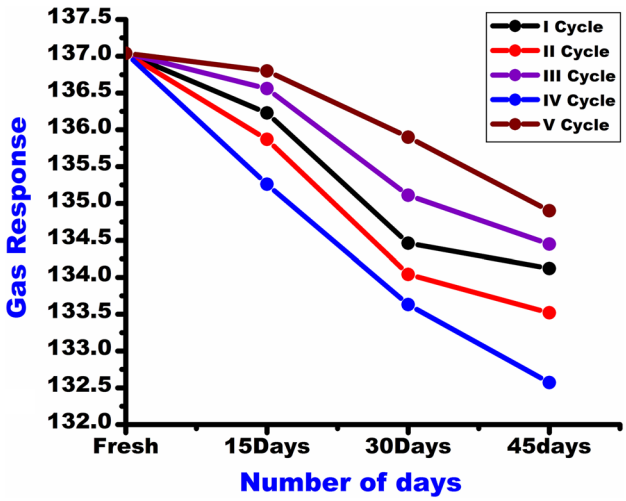

Fig. 11 Reproducibility results for 0.3 M% In^{3+} doped $LaCrO_3$ thick films sensor for petrol vapors at 1000 ppm

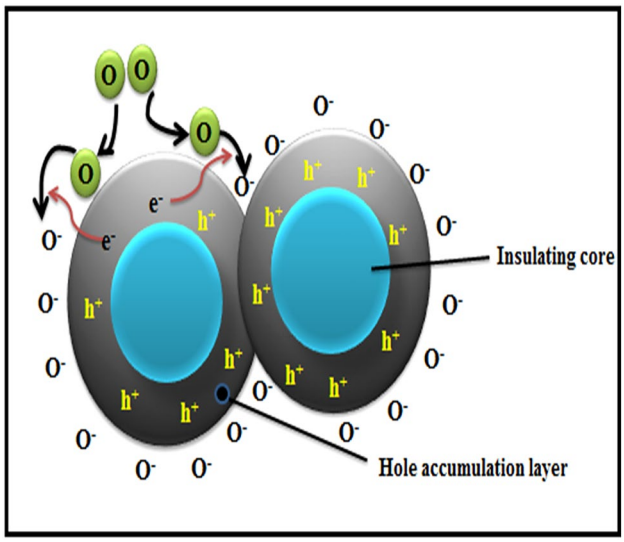

Fig. 12 Gas sensing mechanism of a p-type semiconductor—Formation of insulating region and HAL

of particles and hole accumulation layer near the particle surface [33–35].

The gas sensing mechanism is depending upon the surface of the sensing material. We presumed that the electrons from the valance band of In^{3+} modified $LaCrO_3$ get excited to conduction band near the temperature 100 °C and ready to interact with adsorbed O_2 species to form reduced O_2^- species shown in reaction (1). This generated O_2^- species on the surface of particles plays a vital role during the sensing mechanism when it reacts with petrol vapors. In^{3+} doped $LaCrO_3$ shows better response than undoped $LaCrO_3$ nanostructure because a large amount of O_2^- molecules might

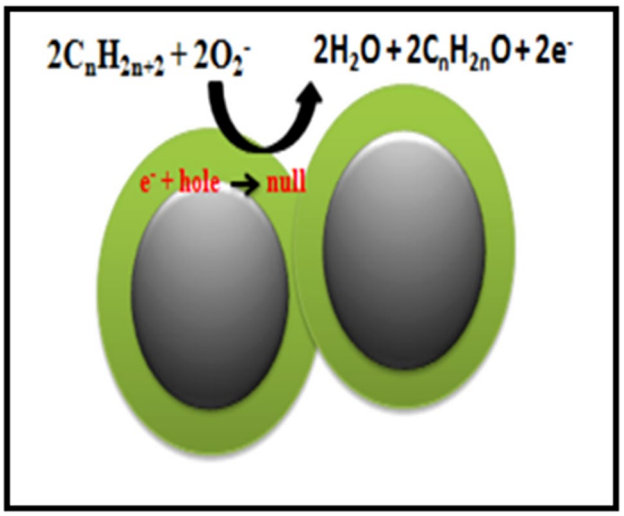

Fig. 13 Gas sensing mechanism of petrol vapours with In^{3+} doped $LaCrO_3$ sensor

be generated on the surface of modified $LaCrO_3$ rather than undoped and also surface area plays an important role during sensing mechanism because the quantity of adsorbed oxygen on the surface of sensing material depends upon the specific surface area of that sensor. It requires a high surface area for the adsorption of a large number of oxygen species. When O_2^- species react with petrol vapors, petrol vapors get oxidized by O_2^- to generate $C_nH_{2n}O$ and H_2O along with the electrons, shown in Fig. 13 and reaction (2).

These released electrons in this entire process will nullify the holes on the surface of In^{3+} doped $LaCrO_3$ and which causes a decrease in the concentration of holes, thereby leading to an increase in resistance of the sensor [36–40].

$$O\ (gas)\ +\ 2e^-\ \rightarrow\ O_2^-(ads) \tag{1}$$

$$2C_nH_{2n+2}\ +\ 2O_2^-\ \rightarrow\ 2H_2O\ +\ 2C_nH_{2n}O\ +\ 2e^- \tag{2}$$

4 Conclusions

The undoped lanthanum chromium oxide and indium doped lanthanum chromium oxide nanostructured material synthesized by cost effective sol–gel process. The $LaCrO_3$ material was doped by varied indium ion concentration from 0.1 M% to 0.7 M%.The thick films all the indium doped $LaCrO_3$ material were fabricated by simple screen printing technique, on glass substrate with the aid of BCA (butyl carbitol acetate) and EC (ethyl cellulose) as binders. The prepared gas sensors characterized by several techniques like XRD, SEM, TEM, EDAX and IR to confirm their structural properties. All the prepared thick film sensors viz. 1 M%

In^{3+} doped $LaCrO_3$, 3 M% $LaCrO_3$, 5 M% $LaCrO_3$, 7 M% $LaCrO_3$ were investigated for gas sensing mechanism for petrol vapours, ethanol, ammonia, NO_2, H2S and CO_2 gases. The modification in $LaCrO_3$ by indium ion enhanced the electrical and sensing properties of $LaCrO_3$. In the overall gas sensing studies it was observed that 0.3 M% In^{3+} doped $LaCrO_3$ sensor showed excellent performance for petrol vapours with 137.04 at 100 ^{0}C. The reason for the high sensitivity may be attributed to effective doping of indium ions in lower concentration over $LaCrO_3$ lattice, leads enhance structural properties, surface area and declined band gap energy. The all concentration of indium doped $LaCrO_3$ sensors showed moderate sensitivity to the other studied gases. The 0.3 M% In^{3+} doped $LaCrO_3$ showed outstanding response and recovery results for petrol vapour sensors with very rapid response and recovery. Most important aspect for the sensor is it's; reproducible results, the reproducibility results conducted for the period of 45 days under identical conditions, the 0.3 M% In^{3+} doped $LaCrO_3$ sensor found to be very consistent for petrol vapour sensing with long term stability and response. The petrol vapour gas sensing mechanism is established for 0.3 M% In^{3+} doped $LaCrO_3$ via hole accumulation layer formation. In overall summary it can be concluded that the 0.3 M% In^{3+} doped $LaCrO_3$ sensor is highly sensitive material for petrol vapour sensing at moderate thermal conditions and can be employed effectively to sense petrol vapours at minimum gas concentration at various gasoline industrial processes.

Acknowledgements Authors gratefully acknowledged to the Physics Department of SPPU University Pune for XRD studies, CIF SPPU, University Pune SEM/EDAX studies. Authors are thankful to STIC Cochin, Kerala, India for TEM results. Authors are also thankful to the instrumentation center of K.T.H.M College, Nashik for FTIR studies. Authors are grateful to Department of Chemistry, L. V. H. College, Panchavati, Nashik, Nano chemistry research laboratory, G. T. P. College, Nandurbar, Department of chemistry Bhosala Military College and Department of Chemistry, Arts, Commerce and Science College, Nandgaon, for providing necessary laboratory facilities for providing necessary laboratory facilities.

Compliance with ethical standards

Conflict of interest Authors declared that they have no conflict of interest regarding the present research in the present article.

References

1. I. Menapace, G. Mera, R. Riedel, E. Erdem, R.A. Eichel, A. Pauletti, G.A. Appleby, J. Mater sci. **43**(17), 5790–5796 (2008)
2. Z. Ju, R. Wei, X. Gao, W. Liu, C. Pang, Opt. Mater. **33**(6), 909–913 (2011)
3. C.D. Entwistle, T.B. Marder, Chem. Mater. **16**(23), 4574–4585 (2004)
4. A. Camposeo, L. Persano, M. Farsari, D. Pisignano, Advanced. Opt. Mater. **7**(1), 1800419 (2019)
5. D. Peng, K. Huang, Y. Liu, S. Liu, H. Wu, Xiao, Polym. Bull. **59**(1), 117–25 (2007)
6. S.G. Shinde, M.P. Patil, G.D. Kim, V.S. Shrivastava, J. Inorg. Organomet. Polym. **30**, 1141–1152 (2019)
7. V.A. Adole, T.B. Pawar, P.B. Koli, B.S. Jagdale, J. Nanostruct. Chem. **9**(1), 61–76 (2019)
8. V.A. Adole, T.B. Pawar, B.S. Jagdale, J. Chin. Chem. Soc. **67**(2), 306–315 (2020)
9. V.A. Adole, R.A. More, B.S. Jagdale, T.B. Pawar, S.S. Chobe, Chem. Sel. **5**(9), 2778–2786 (2020)
10. K. Tao, X. Han, D. Yin, L. Wang, L. Han, L. Chen, Nanomater. Polym. **2**, 10918–10925 (2017)
11. J. Lelieveld, K. Klingmüller, A. Pozzer, U. Pöschl, M. Fnais, A. Daiber, T. Münzel, Eur. Heart J. **40**(20), 1590–1596 (2019)
12. S.G. Patil, A.V. Patil, C.G. Dighavkar, K.S. Thakre, R.Y. Borse, S.J. Nandre, N.G. Deshpande, R.R. Ahire, Front. Mater. Sci. **9**(1), 14–37 (2015)
13. V.V. Deshmane, A.V. Patil, Mater. Res. Express **6**, 025904 (2019)
14. B.A. Murtala, Z.A. Wan, A.S. Siti, S.A. Boon, Malays J Med Sci. **22**(1), 23–31 (2015)
15. R.S. Mane, H.M. Pathan, C.D. Lokhande, S.H. Han, Sol. Energy **80**(Suppl. 2), 185–190 (2006)
16. D. Zhang, Z. Liu, C. Li, T. Tang, X. Liu, S. Han, B. Lei, C. Zhou, ACS Nano. Lett. **4**(10), 1919–1924 (2014)
17. P.D.C. King, T.D. Veal, F. Fuchs, Y. Wang, D.J. Payne, A. Bourlange, H. Zhang, G.R. Bell, V. Cimalla, O. Ambacher, R.G. Egdell, F. Bechstedt, F. Conville, J. Phys. Rev. B **79**, 205201–205211 (2009)
18. D. Zhang, C. Li, S. Han, S. Liu, T. Tang, C. Zhou, J. Adv. Mater. **15**, 143–145 (2003)
19. H. Kim, A. Pique, J.S. Horwitz, H. Mattoussi, H. Muratta, Z.H. Kafafi, D.B. Chrisey, Appl. Phys. Sci. Lett. **74**, 3444–3446 (1999)
20. S.V. Shinde, C.P. Sawant, K.H. Kapadnis, J. Nanostruct. Chem. **9**, 231–245 (2019)
21. C. Li, D.H. Zhang, S. Han, X.L. Liu, T. Tang, C.W. Zhou, Adv. Mater. **82**, 143–146 (2003)
22. Q. Liu, W. Lu, A. Ma, J. Tang, J. Lin, J. Fang, World J. Am. Chem. Soc. **127**, 5276–5277 (2005)
23. B.X. Li, Y. Xie, M. Jing, G.X. Rong, Y.C. Tang, G.Z. Zhang, Langmuir **22**, 9380–9385 (2006)
24. D. Yu, S.H. Yu, S. Zhang, J. Zuo, D. Wang, Y.T. Quin, Adv. Func. **13**(6), 497–501 (2003)
25. Z. Li, Y. Fan, J. Zhan, Interface Sci. 3348–3353 (2010)
26. R.P. Patil, C. Hiragond, P.V. More, G.H. Jain, P.K. Khanna, V.B. Gaikwad, Vaccum **146**, 455–461 (2019)
27. Y. Xu, D. Sun, H. Hao, D. Gao, Y. Sun, RSC Adv. **6**, 98994–99002 (2016)
28. S. Mondal, M. Kumari, R. Madhuri, P.K. Sharma, Appl. Phys. A **123**(494), 1–15 (2017)
29. M. Siemons, A. Leifter, U. Simon, Adv. Funct. Mater. **17**, 2189–2197 (2007)
30. P.B. Koli, K.H. Kapadnis, U.G. Deshpande, J. Nanostruct. Chem. **9**(2), 95–110 (2019)
31. B. Senthilkumar, R.K. Selvan, P. Vinothbabu, I. Perelshtein, A. Gedanken, J. Mater. Chem. Phys **130**, 285–292 (2011)
32. V.S. Shinde, K.H. Kapadnis, C.P. Sawant, J. Nanostruct. Chem. **9**(3), 231–245 (2019)
33. M.K. Deore, G.H. Jain, Int. J. Nano **7**(1), 57–72 (2014)
34. J. Qi, H. Zhang, S. Lu, X. Li, M. Xu, Y. Zhang, J. Nanomater. **1–6** (2014)
35. Q. Tang, X. Hu, M. He, L. Xie, Z. Zhu, J. Wu, J. Appl. Sci. **8**(1091), 2–14 (2018)
36. H.J. Kim, J.H. Lee, J. Sens. Actuators B **192**, 607–627 (2014)

37. M.S. Gabriel, H.F. Emerson, J.N. Eduardo, J.C. Katia, S.C. Paulo, Quimi. Nov. **35**, 1–12 (2012)
38. Fujita, P – Type oxide semiconductor and method for manufacturing same Patent Application Publication 23, US 2019 / 0157380 A1 (2019)
39. P.B. Koli, K.H. Kapadnis, U.G. Deshpande, J. Environ. **7**(5), 103373 (2019)
40. P.B. Koli, K.H. Kapadnis, U.G. Deshpande, J. Nanostruct. Chem. **8**(4), 453–463 (2018)